metals

MDPI

Article

Microstructure and Mechanical Properties of the TC4 Alloy Obtained by Equal-Channel Angular Pressing in Combination with Reversible Hydrogen Alloying

Irina P. Semenova [1,*], Luiza R. Rezyapova [1], Alexander V. Polyakov [1], Yuecheng Dong [2], Zhonggang Sun [2] and Igor V. Alexandrov [1]

[1] Department of Materials Science and Metal Physics, Ufa University of Science and Technology, 32 Zaki Validi St., 450076 Ufa, Russia; luiza.rezyapova.97@mail.ru (L.R.R.); alex-v.polyakov@mail.ru (A.V.P.); igorvalexandrov@yandex.ru (I.V.A.)

[2] College of Materials Science and Engineering/Tech Institute for Advanced Materials, Nanjing Tech University, Nanjing 211816, China; dongyuecheng@njtech.edu.cn (Y.D.); sunzgg@njtech.edu.cn (Z.S.)

* Correspondence: semenova-ip@mail.ru

Abstract

This paper studies the effect of reversible hydrogen alloying of the TC4 alloy on the microstructure, phase composition, and mechanical properties before and after equal-channel angular pressing. It is shown that the introduction of 0.3% hydrogen followed by quenching from a temperature of 850 °C leads to the formation of a thin-plate α″-martensite, which made it possible to implement 6 passes (ε ~ 4.2) of pressing at 600 °C. As a result of the deformation of the TC4-H alloy and subsequent thermal vacuum treatment to remove hydrogen, an ultrafine-grained structure with an average size of the α-phase of 0.15 μm was formed, which led to strengthening of the alloy to 1490 MPa with a relative elongation of about 5% at room temperature. The reasons for a more significant refinement of the grain/subgrain structure and an increase in the tensile strength of the hydrogenated alloy after equal-channel angular pressing in comparison with hydrogen-free TC4 alloy are discussed.

Keywords: titanium alloy; reversible hydrogen alloying; equal-channel angular pressing; ultrafine-grained structure

check for updates

Academic Editor: Dmitri Molodov

Received: 19 June 2025
Revised: 23 July 2025
Accepted: 26 July 2025
Published: 27 July 2025

Citation: Semenova, I.P.; Rezyapova, L.R.; Polyakov, A.V.; Dong, Y.; Sun, Z.; Alexandrov, I.V. Microstructure and Mechanical Properties of the TC4 Alloy Obtained by Equal-Channel Angular Pressing in Combination with Reversible Hydrogen Alloying. *Metals* **2025**, *15*, 839. https://doi.org/10.3390/met15080839

Copyright: © 2025 by the authors. Licensee MDPI, Basel, Switzerland. This article is an open access article distributed under the terms and conditions of the Creative Commons Attribution (CC BY) license (https://creativecommons.org/licenses/by/4.0/).

1. Introduction

It is known [1,2] that hydrogen in titanium and its alloys forms an interstitial solution and causes hydrogen embrittlement of materials. Hydrogen embrittlement is most pronounced in pure titanium and single-phase titanium alloys with an α-structure. Embrittlement is associated with the formation of a hydride phase, which significantly reduces the tensile strength of the material. In two-phase alloys, the formation of hydrides is prevented by the presence of a β-phase capable of dissolving hydrogen. However, in such alloys, zones supersaturated with hydrogen can form [2], which leads to brittle fracture under slow deformations, such as long-term static (strain rate 10^{-3}–10^{-4} s^{-1}) or slow dynamic loadings.

The effect of hydrogen on (α + β) titanium alloys is determined by the ratio of phases in their microstructure. At an increased concentration of the β-phase, hydrogen predominantly migrates within the crystal lattice of the β-phase and reacts with the α-phase at the α/β interfaces. The α/β boundary itself is considered an effective hydrogen sink [3–5] and a place for the formation of hydride inclusions caused by excess hydrogen solubility

in the α-phase [6]. The formation of such inclusions significantly deforms the structure of the alloy, which contributes to its embrittlement due to the weakening of the α/β-phase interfaces by the hydride phase [7].

However, when properly used as a temporary alloying element, hydrogen can significantly improve the machinability, microstructure, and mechanical properties of titanium alloys [8,9]. Thermohydrogen treatment is based on the modifying effect of hydrogen as an alloying element on the phase compositions, development of metastable phases, and kinetics of phase transformations in titanium alloys [4–8]. Hydrogen is a unique alloying element in titanium alloys because, unlike other elements, it can be easily added and removed without melting.

For example, the use of preliminary hydrogenation before severe plastic deformation (SPD) allows for an increase in the deformation capacity of the material [10–13]. In particular, in the experiments [12,13] using the Ti-6Al-4V alloy, it was shown that when using hydrogen as a temporary alloying element in the process of forming an ultrafine-grained/submicrocrystalline structure by the methods of all-round pressing in two-phase titanium alloys, phase transformations occur that facilitate the refinement of the structure. This allows for the reducing of the deformation degree necessary to obtain a microstructure in the alloy with a grain/subgrain size in the α-phase of 0.1–0.5 μm.

At the same time, the all-round pressing method has a fairly simple deformation scheme compared, for example, to equal-channel angular pressing (ECAP), in which shear deformation is realized in the deformation zone [14,15]. The ECAP method for titanium alloy billets can be implemented only at elevated temperatures. For example, the Ti-6Al-4V (similar to Russian VT6) alloy was subjected to ECAP with an increased channel intersection angle (120° and 135°) at a temperature of 700 °C [16,17]. In recent studies, two-phase VT6 and VT8M-1 alloys were successfully deformed at temperatures of 650 °C [18] and 750 °C [19]. The tensile strength of the alloys after ECAP usually increased by about 25% due to the formation of a grain size of about 0.5 μm [16]. Reduction of the temperature of deformation treatment by the ECAP method to 600 °C was demonstrated for the Ti-6Al-4V ELI alloy with an extra low content of impurities, in particular, oxygen [16]. It can be assumed that the use of preliminary alloying of the TC4 alloy with hydrogen will allow, on the one hand, an increase in the deformation capacity of the material during shear deformation during the ECAP process, and on the other hand, the attainment of a higher strength with a decrease in the accumulated degree of deformation.

The aim of this work is to study the effect of hydrogen alloying on the structural-phase composition and mechanical properties of the TC4 alloy, the deformation capacity during ECAP to form an ultrafine-grained (UFG) structure, and the increase in strength of various properties.

2. Materials and Methods

For the study, titanium TC4 alloy rods with a square cross-section of 12 mm with the elemental composition of the material Ti-6Al-4V (Ti-6.3Al-4.2V-0.3Fe-0.1O-0.04Si-0.02N-0.01C, in wt%) were obtained. These rods were subjected to hydrogen-imbued annealing at the temperature of 750 °C and air cooling to attain a concentration of H = 0.3%. Then, subsequent quenching from 850 °C in water at a cooling rate of more than 50 °C/s was carried out.

When choosing the hydrogen concentration, we were guided by previously published data [20,21] which showed that at a hydrogen concentration of less than 0.3 wt%, α′-martensite is formed mainly in an alloy of type Ti-6Al-4V. At concentrations above 0.3 wt%, α′-phase is transformed to α″-phase, which is identical to the transformation of titanium during alloying with β-isomorphic stabilizers [12]. It is expected that the formation of α″-martensite in the microstructure makes it possible to reduce the flow stress

during deformation of the alloy by the ECAP method. The choice of the studied hydrogen concentration of approximately 0.3 wt% was also due to a decrease in the probability of hydride formation at grain boundaries. For example, in [22] it was shown that in the VT6 alloy, with an increase in the hydrogen content of more than 22 wt%, the alloy retains a two-phase state and, when deformed at 700 °C, hydrides are released.

Upsetting tests of hydrogenated samples were carried out in the temperature range of 500–800 °C with a step of 50 °C and initial deformation rates of 10^{-2}, 10^{-3}, and 10^{-4} s^{-1}. For a statistical analysis, three samples were tested in each test mode. For each test, 7 mm high samples were made. The manufacturing accuracy was controlled by measuring with a caliper with a measurement error of 0.01 mm. The upsetting was carried out to a deformation degree of 80% (final height of samples $\approx 1.5 \pm 0.2$ mm) and was controlled by software Bluehill Universal (version 4.08.24426) by moving the crosshead by a specified value (Table 1). Tests at 500 °C and an initial strain rate of 10^{-2} were stopped prematurely due to a sharp drop in stress caused by the appearance of cracks in the samples. Tests at 650 °C and an initial strain rate of 10^{-4} s^{-1} were similarly stopped.

Table 1. Parameters of samples TC4-0.3H before and after upsetting.

Temperature (°C)	Initial Deformation (s^{-1})	Initial Height (mm)	Final Height (mm)	Deformation (%)
500	10^{-2}	7.04	4.87	30
	10^{-3}	7.04	1.27	82
	10^{-4}	7.05	1.1	84
550	10^{-2}	7.07	1.12	84
	10^{-3}	7.09	1.14	84
	10^{-4}	7.05	1.1	84
600	10^{-2}	7.09	1.52	79
	10^{-3}	7.07	1.52	79
	10^{-4}	7.05	1.52	78
650	10^{-2}	6.99	1.5	79
	10^{-3}	7.07	1.52	79
	10^{-4}	7.05	3.51	50
700	10^{-2}	7.07	1.12	84
	10^{-3}	7.01	1.37	80
	10^{-4}	7.0	1.05	85
750	10^{-2}	7.07	1.52	79
	10^{-3}	7.07	1.52	79
	10^{-4}	7.08	1.52	79
800	10^{-2}	7.05	1.1	84
	10^{-3}	7.05	1.3	82
	10^{-4}	7.0	1.05	85

Hydrogenated billets with a diameter of 12 mm were subjected to ECAP under isothermal conditions at a temperature of 600 °C (tooling temperature T = 530 °C) along the Bc route (turning the rod around its longitudinal axis by 90 degrees in the same direction after passing it through the ECAP die set) on a tooling with a channel intersection angle of 120° at a

deformation rate of 10^{-3} s^{-1}. The maximum number of passes without destruction of the material was 6 cycles, which corresponds to a deformation degree of $\varepsilon \sim 4.2$.

The microstructure of the samples was studied using an Olympus GX53 (Olympus Corporation, Tokyo, Japan) optical microscope, a JEOL JSM-6490LV (JEOL, Tokyo, Japan) scanning electron microscope (SEM) at an accelerating voltage of 20 kV, and a JEOL JEM-2100 (JEOL, Tokyo, Japan transmission electron microscope (TEM) operating at an accelerating voltage of 200 kV. Foils for studying the fine structure were obtained by mechanical thinning of the blanks on grinding paper to a thickness of 0.1–0.2 mm, followed by electrolytic polishing on a Tenupol-5 (Struers, Denmark) unit using an electrolyte of the following composition: 300 mL methanol (CH_3OH), 175 mL butanol (C_4H_9OH), and 30 mL perchloric acid ($HClO_4$). The sizes of structural elements were measured by the secant method.

X-ray phase analysis (XRD) was performed on a Bruker D2 Phaser (Bruker corporation, Billerica, MA, USA) diffractometer with CuKα radiation (λ = 0.1540562 nm) within the scattering angles 2θ from 25° to 95°.

Microhardness values were measured on an EmcoTest "DuraScan-50" «EMCO-TEST PrufmaSchinen GmbH», Kuchl, Austria) automatic microhardness tester using the Vickers method by pressing a regular diamond pyramid with an apex angle of 136° into the test sample. The maximum applied load on the indenter was 100 g and the holding time was 10 s.

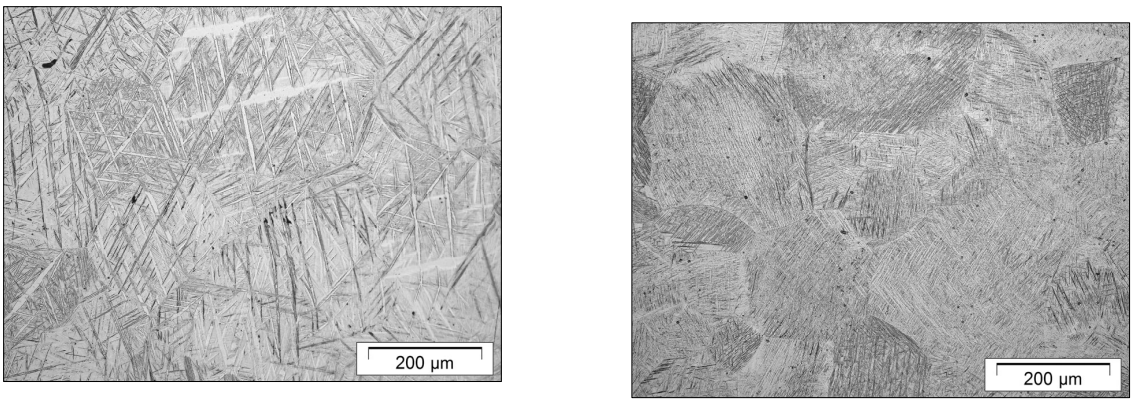
The mechanical properties of the samples were assessed using standard round samples with a diameter of 3 mm. Mechanical tensile tests were carried out at room temperature with an initial deformation rate of 10^{-3} s^{-1}.

3. Results

3.1. The Effect of Hydrogen Alloying on the Microstructure of the TC4 Alloy

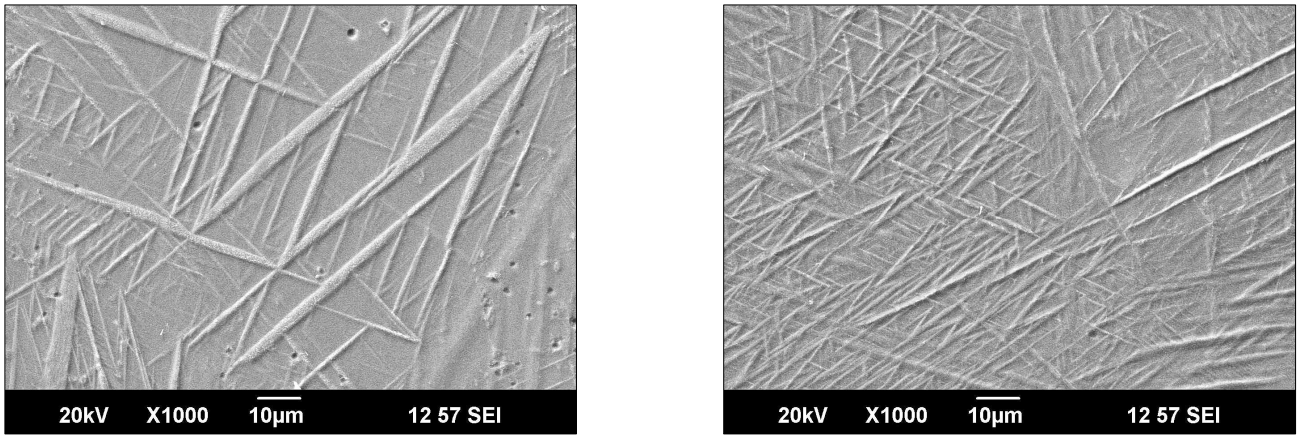
The microstructure in the initial state was characterized by a mixed structure consisting of a fraction of grains of the primary α-phase (25%) and a β-transformed α + β component. The grains had a slight elongation: the average length was 14.7 ± 3.1 μm and the width was 7.8 ± 1.5 μm. The microhardness in the initial state was 348 HV.

After hydrogenation, a martensitic structure was formed (Figure 1). A comparative analysis of the structure in the transverse and longitudinal directions made it possible to establish its homogeneity, i.e., the structure of the material in the center and at the surface layers closer to the edge is identical. In the longitudinal direction (Figure 1b), large polyhedral grains with sizes from 50 to 500 μm are more clearly observed, inside which several packets of plates are fixed (Figure 2).



(**a**) (**b**)

Figure 1. Microstructure of TC4-0.3H alloy: (**a**) the billet cross-section; (**b**) the longitudinal billet section. Optical metallography.

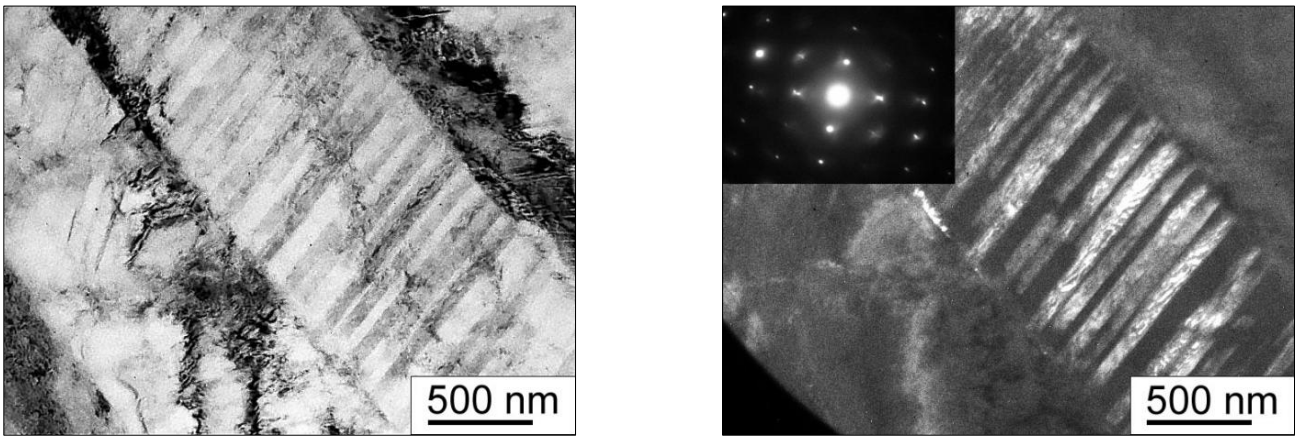


(**a**) (**b**)

Figure 2. SEM microstructure of TC4-0.3H alloy: (**a**) the billet cross-section; (**b**) the longitudinal billet section. Scanning electron microscopy.

The plates, collected in colonies and located in the body of the grains, have different thicknesses (Figure 2). The thickness of the plates varies in the range from 0.3 to 4.0 μm.

A study of the microstructure using a transmission electron microscope showed that the observed plates are a collection of more dispersed, regularly arranged plates or twins, the thickness of which does not exceed 100 nm (Figure 3). The presence of twins is also confirmed by the diffraction pattern with extra reflections present on it (Figure 3b).



(**a**) (**b**)

Figure 3. Microstructure of TC4-0.3H alloy: (**a**) bright field; (**b**) dark field. Transmission electron microscopy.

Figure 4 shows the X-ray diffraction patterns of the alloy before and after hydrogen alloying. The hydrogen-free alloy has a typical phase composition characterized by peaks of the α and β phases. The X-ray diffraction pattern shows peaks of the martensitic α″-phase after hydrogen alloying.

The addition of hydrogen causes a large distortion in the lattice, which increases the resistance to shear displacement during the martensitic transformation and leads to a change in the crystal structure from the hcp to the orthorhombic lattice [6]. Thus, the structure of the alloy after hydrogenation is represented by α″ martensite needles in the β-phase grains.

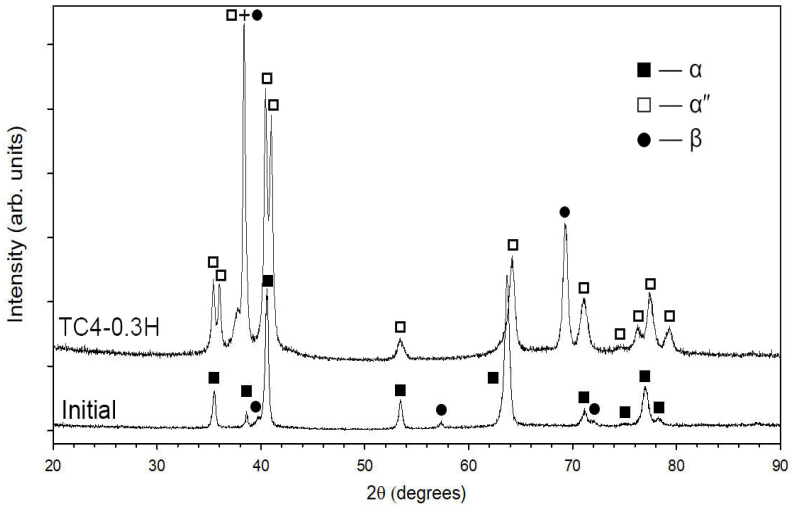


Figure 4. X-ray diffraction pattern of initial TC4 and TC4-0.3H alloys.

3.2. Evaluation of the Deformability of Hydrogenated TC4-0.3H Alloy by the Isothermal Upsetting Method

As is known, the implementation of multi-pass ECAP in alloys such as Ti-6Al-4V is associated with certain difficulties, primarily with its low deformability. This method is characterized by a narrow deformation focus zone and its high intensity. In our early works [16], an increase in the deformability of the alloy during ECAP was achieved using an elevated processing temperature of up to 700 °C and using tooling with increased channel intersection angles of 120° and 135°.

To assess the deformation behavior of the hydrogenated TC4 alloy, rheological upset tests were carried out in the temperature range of 500–800 °C with a step of 50 °C with different strain rates. Typical stress-strain curves are shown in Figure 5.

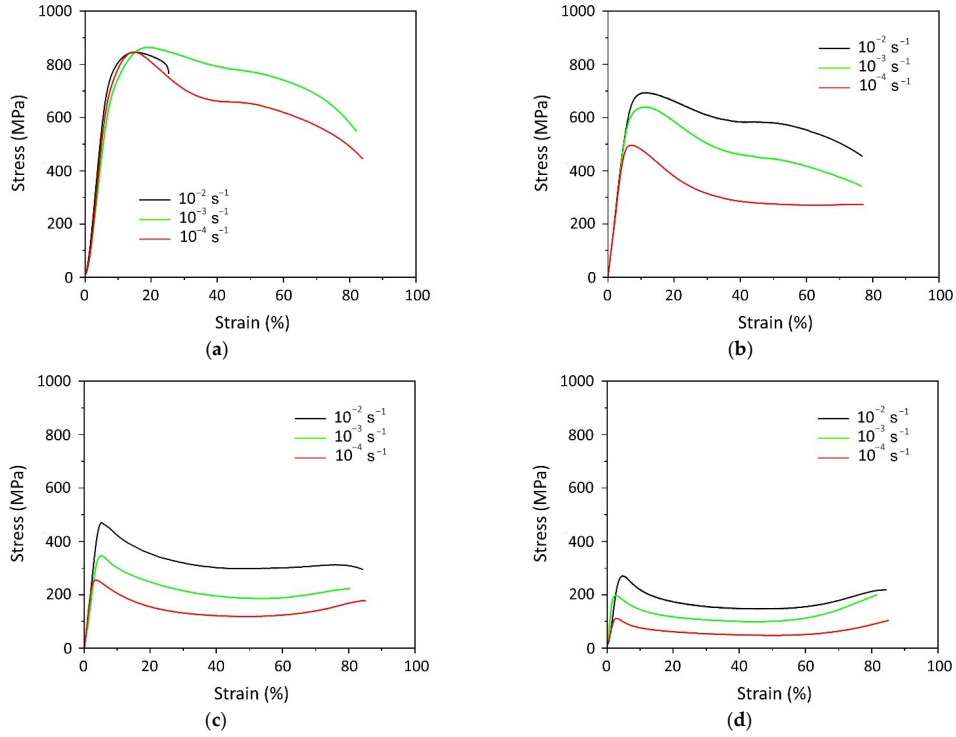


Figure 5. Typical stress-strain curves of TC4-0.3H alloy during upsetting at a temperature of: (**a**) 500 °C; (**b**) 600 °C; (**c**) 700 °C; (**d**) 800 °C.

In the curves, regardless of the test mode of the samples, it is possible to distinguish an elastic region and a softening region, which occurs immediately after reaching the yield strength. In Figure 6 and Table 2, the test results are summarized in graphs of the yield strength of the hydrogenated alloy as a function of temperature and strain rate. With a decrease in the initial strain rate and an increase in the test temperature, a decrease in the flow stress value was observed.

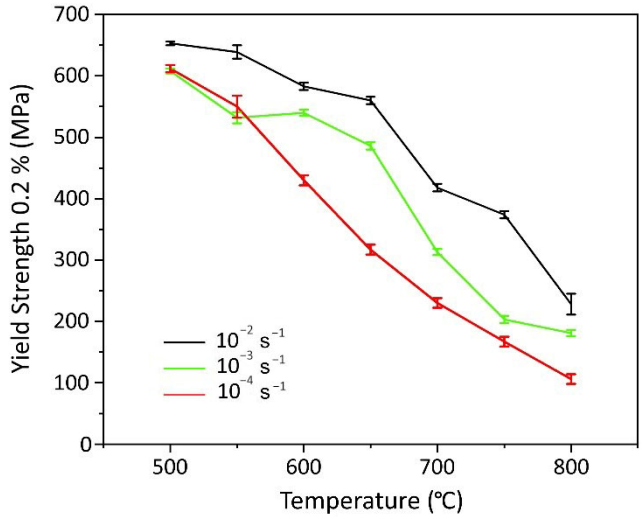


Figure 6. Dependence of the yield strength on temperature and strain rate of the TC4-0.3H alloy under compression.

Table 2. Yield strength of the TC4-0.3H alloy under compression.

Yield Strength 0.2% (MPa)							
Strain Rate, $\dot{\varepsilon}$ \ Temperature, (°C)	**500**	**550**	**600**	**650**	**700**	**750**	**800**
$\mathbf{10^{-2}}$	653 ± 3	639 ± 11	583 ± 7	560 ± 5	418 ± 9	374 ± 4	228 ± 17
$\mathbf{10^{-3}}$	608 ± 4	532 ± 9	540 ± 10	486 ± 8	313 ± 7	203 ± 8	181 ± 5
$\mathbf{10^{-4}}$	612 ± 6	550 ± 18	430 ± 8	317 ± 12	230 ± 8	167 ± 11	106 ± 7

The highest yield strength values (above 800 MPa) of the alloy were observed during tests at 500 °C (Figure 5a). The flow stresses at 600 and 700 °C were in the range of 540–350 MPa at an average strain rate of 10^{-3} s^{-1} (Figure 5b,c). Similar deformation behavior was observed for a conventional hydrogen-free alloy; therefore, the recommended temperature range for deformation of TC4-0.3H alloy samples by the ECAP method can also be 600–700 °C at a strain rate of about 10^{-3} s^{-1} [22]. The deformation temperature of 800 °C is at the threshold of recrystallization onset, and under intense action, dynamic recrystallization is possible, which can lead to structural heterogeneity [16].

Based on the experiment, defect-free billets were obtained after 6 passes ($\varepsilon \sim 4.2$) at 600 °C on an ECAP tool with a channel intersection angle of 120° (Figure 7).

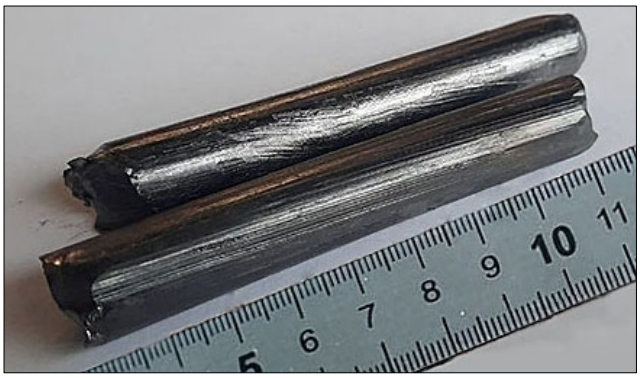
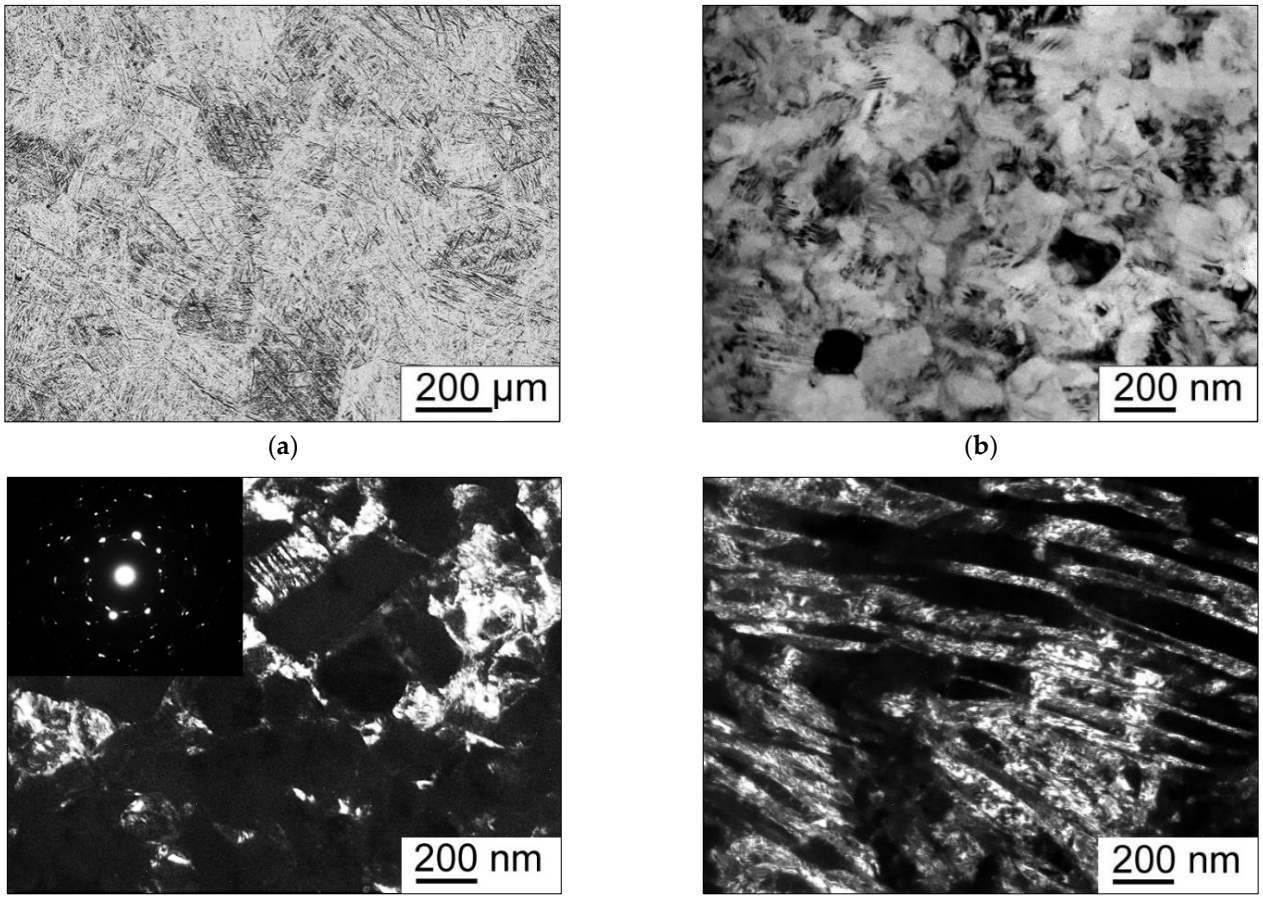


Figure 7. View of hydrogenated blanks made of TC4-0.3H alloy after 6 passes of ECAP.

3.3. Microstructure of TC4-0.3H Alloy After ECAP

The previously observed distinct boundaries of polyhedral β-grains were not revealed (Figure 8a). ECAP of the hydrogenated material resulted in the formation of an ultrafine-grained two-phase α + β structure with a grain/subgrain size of 150 ± 30 nm (Figure 8b,c). However, local zones are observed where the lamellar structure and twins are preserved, which is confirmed by the electron diffraction patterns (Figure 8c,d). The presence of such local zones can probably be explained by the shear deformation pattern of ECAP, in contrast to, for example, all-round isothermal forging [15].



(**a**) (**b**) (**c**) (**d**)

Figure 8. Microstructure of the TC4-0.3H + ECAP alloy: (**a**) optical metallography; (**b**) TEM, bright field; (**c**,**d**) TEM, dark field.

The results of X-ray phase analysis (Figure 9) confirm the fact of the formation of a two phase (α + β) structure based on the decomposition of the metastable α″-phase and the diffusion redistribution of alloying elements: in depleted microvolumes, the equilibrium α-phase was released, retaining the lamellar structure, and in enriched ones, the β-phase.

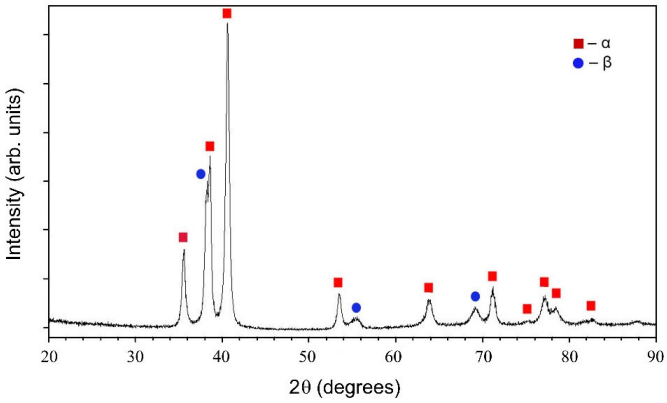


Figure 9. X-ray pattern of the TC4-0.3H + ECAP alloy.

The microhardness evaluation of the samples showed that there is a slight change in the values over the cross-section of the rod, which indicates uniform deformation of the material throughout the volume of the billet. The average microhardness value was 360 ± 10 HV.

To remove hydrogen from the material, annealing was used in a vacuum environment for 1 h at a temperature of 550 °C. The material retained its heterogeneous structure observed after ECAP (Figure 10a). In this case, the microhardness of the material increased to 430 HV. A slight increase in microhardness may be associated with the decomposition of the metastable β-phase and the release of secondary, more dispersed particles of the α-phase [23]. This is evidenced by the formation of very small grains less than 50 nm in size (Figure 10b–d).

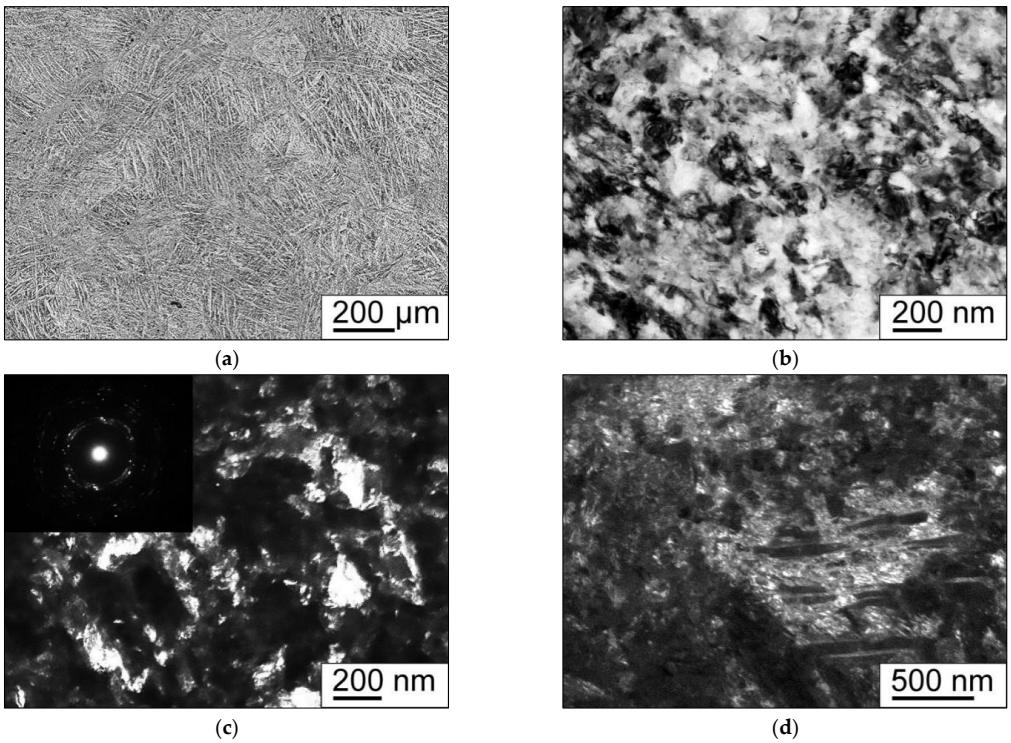


Figure 10. Microstructure of the TC4-0.3H + ECAP alloy after vacuum annealing: (**a**) optical metallography; (**b**) TEM, bright field; (**c**,**d**) TEM, dark field.

It should be noted that the azimuthal blurring of reflections in the electron diffraction pattern after annealing (Figure 10c) is reduced compared to that in the ECAP state (Figure 8c), which may qualitatively indicate a reduction in internal elastic stresses after annealing due to the processes of recovery and redistribution of dislocations.

3.4. Mechanical Properties of the TC4 and TC4-0.3H + ECAP Alloys

Figure 11 and Table 3 show typical tensile curves of samples and mechanical properties in the studied structural states of the TC4 alloy.

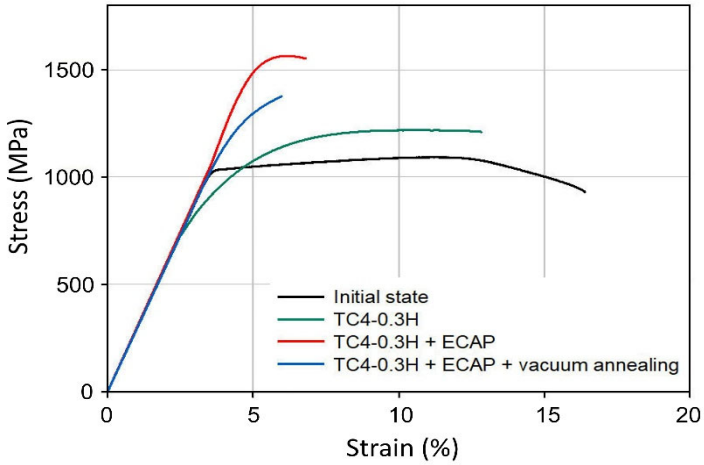


Figure 11. Tensile stress-strain curves of the TC4 alloy in different structural states.

Table 3. Mechanical properties of the TC4 alloy at room temperature.

States	HV	UTS (MPa)	0.2YS (MPa)	ε (%)
Initial	348	1083 ± 25	1037 ± 15	13.0 ± 2.2
TC4-0.3H	320 ± 6	1218 ± 29	799 ± 5	8.0 ± 2.0
TC4-0.3H + ECAP	361 ± 10	1550 ± 10	1440 ± 10	2.5 ± 0.5
TC4-0.3H + ECAP + vacuum annealing	430 ± 17	1493 ± 10	1214 ± 10	4.3 ± 0.5

In Figure 11, the tensile stress-strain curve for the alloy in the initial state is typical for two-phase titanium alloys. After reaching the yield point (1037 ± 12 MPa), a slight strengthening of the material is observed with an exit strength of 1083 ± 25 MPa, after which localization of the deformation occurs with the formation of a "neck" and subsequent failure. Uniform elongation was 13 ± 2.2%.

Subsequent hydrogenation resulted in a significant decrease in the yield strength of the material to 799 MPa, which probably had some influence on the reduction in the microhardness of the material from 360 to 320 HV (see Table 3). At the same time, a significant increase in the ultimate strength to 1218 MPa was observed, and the relative elongation averaged 8% (Figure 11, Table 3). It is also worth noting the change in the nature of the loading curve: after reaching the yield strength, a stage of intensive hardening is observed with an exit to a platform (the stage of steady-state flow of the material), where the maximum stress values (ultimate strength) are observed (Figure 11).

The formation of the UFG structure after ECAP resulted in significant strengthening to 1550 MPa, while the conditional yield stress increased almost two times (1440 MPa) compared to that in the hydrogenated state. In this case, the relative elongation was about 2.5% (Figure 11, Table 3). After reaching the maximum stress, brittle fracture of the samples occurs without localization of deformation. Vacuum annealing at 550 °C after

ECAP had a positive effect on the mechanical properties. On the one hand, an increase in microhardness was observed from 360 to 430 HV and the tensile strength remained unchanged at 1500 MPa, apparently due to the aging processes occurring during annealing at 550 °C [23,24]. At the same time, the preservation of high strength was accompanied by an increase in relative elongation to 5.0 ± 0.5% (Figure 11, Table 3). The increase in the plasticity of the material may be associated with competing recovery processes during heating due to the redistribution and annihilation of dislocations.

4. Discussion

4.1. Microstructure and Mechanical Properties of the TC4 Alloy After Thermal Hydrogen Treatment

The study of the TC4 alloy microstructure after hydrogenation showed the formation of a typical martensite-type structure, which consisted of large polyhedral grains (from 50 to 500 μm), inside which packets of martensite plates with thicknesses of 0.2 to 4.0 μm were observed (Figures 1 and 2). Thus, the introduction of 0.3% hydrogen into the alloy transfers the alloy to a single-phase β-state, and upon subsequent cooling by quenching from 850 °C, packets of martensite plates are formed [3]. It should be noted that under these conditions, α''-martensite is formed, as evidenced by the corresponding peaks in the X-ray diffraction pattern in Figure 4. As reported in [12], the process of α''-martensite formation is identical to the $\alpha' \rightarrow \alpha''$ transformation upon alloying with β-isomorphic stabilizers. As has been shown, α''-martensite plates are a collection of dispersed, regularly arranged plates or twins, which is confirmed by bright-field TEM images and electron diffraction patterns in the present study (Figure 3).

When examining the mechanical behavior of the alloy before and after hydrogen annealing, it was found that the tensile strength of the alloy increased from 1083 to 1218 MPa, while the yield strength and relative elongation significantly decreased from 1037 to 800 MPa and from 13 to 8%, respectively. Obviously, this is due to the formation of a martensitic structure and is consistent with the results of various researchers under similar conditions of thermal hydrogen treatment of the Ti alloy [3,6,7,12,13]. As noted earlier, in two-phase titanium alloys, at such a low hydrogen concentration (up to 0.3%), titanium hydrides are not formed due to the presence of the β-phase, which dissolves hydrogen well, which prevents brittle fracture of the alloy; however, local zones supersaturated with hydrogen relative to the solid solution may occur, contributing to brittle fracture at low deformation rates [10].

4.2. Microstructure and Mechanical Behavior of the TC4-0.3H Alloy After ECAP

As shown by the present study, thermal hydrogen treatment of the TC4 alloy did not reduce the deformability of the alloy during ECAP, although the microstructure of the alloy was characterized by a lamellar structure (Figure 2), which significantly reduces the deformability of the alloy in the temperature range of 600–700 °C [22]. This can probably be explained by the formation of dispersed α''-martensite with an ortho-rhombic crystal lattice in the alloy, which is known to be noticeably "softer" than α'-martensite [13]. An increase in the technological plasticity of the hydrogenated VT6 alloy during severe plastic deformation by all-round forging was noted in [12,13]. Thus, the hydrogenated alloy was successfully deformed in the ECAP tooling in 6 passes, achieving a total deformation degree of $\varepsilon \sim 4.2$ at 600 °C without the formation of defects (Figure 8). In this work, after ECAP treatment, the microstructure of the TC4 alloy underwent a refinement of martensite plates with the formation of equiaxed α and β particles with a particle size of 0.15 ± 0.03 μm (Figure 8). In this case, thermal hydrogen treatment had a positive effect on the formation of the UFG structure in the alloy during ECAP, while the minimum size of the α phase

of 0.3 μm was obtained in the hydrogen-free Ti-6Al-4V ELI alloy only after ECAP and extrusion [24]. After ECAP at 600 °C in hydrogen-free alloy VT6, a UFG structure with an α and β-phase particle size of 0.4–0.6 μm on average was observed [16,17].

As was shown in [13], using the example of two-phase titanium alloy VT9, hydrogen alloying leads to a decrease in the size of the initial β-grains, an increase in the volume fraction of the β-phase, a decrease in the thickness of the α-phase plate, and a significant increase in the interplate distance occupied by the β-phase. The transformation of the lamellar microstructure into an equiaxed one during subsequent deformation at relatively low temperatures (up to 600 °C) occurs due to the accumulation of defects in the phases, subsequent polygonization and/or) recrystallization of the phases, and fragmentation of the plates along the transverse boundaries with their subsequent spheroidization [25,26]. In this regard, strengthening of the β-phase obtained as a result of alloying with hydrogen creates favorable conditions for the accumulation of defects and the emergence of disoriented fragments. In this case, the combination of the processes of decomposition of the β-phase and deformation can lead to an additional increase in the dispersion of the precipitated α-phase [13]. For example, in the hydrogenated alloy VT6 after upsetting by 80% at a temperature of 600 °C [12], a submicrocrystalline structure with an equiaxed grain/subgrain size of 0.18 μm was obtained by the method of all-round isothermal forging. The ultimate strength of hydrogenated samples after ECAP increased significantly to 1550 MPa, and the yield strength from 800 to 1440 MPa. It should be noted that in the VT6 and Ti-6Al-4V ELI alloys, after 4–10 ECAP passes, it was possible to achieve a strength of approximately 1200 MPa [17]. Such a significant strengthening of the hydrogenated alloy can apparently be explained by a stronger refinement of the structure after SPD. After ECAP at 600 °C, a UFG structure with an average particle size of α and β-phase 0.4–0.6 μm was observed in the hydrogen-free VT6 alloy [16,17], whereas after ECAP, it was possible to obtain a particle size of up to 0.15 μm in the hydrogenated alloy. Obviously, an additional contribution to grain refinement during ECAP at 600 °C of a hydrogenated alloy is provided by $\alpha'' \rightarrow \beta$ phase transformations, which lead to the appearance of new boundaries and, as a consequence, to a decrease in the size of the elements of the grain-subgrain structure [27]. As was shown in [27], the rearrangement of the bcc lattice in the hcp in titanium and its alloys during the $\alpha'' \rightarrow \beta$ phase transformation is accompanied by shear deformation, the value of which reaches 0.2–0.3. However, the relative elongation was small (up to 2.5%), which is apparently due to high internal elastic stresses, as evidenced by the azimuthal blurring of reflections on the electron diffraction pattern (Figure 8c). Thus, during ECAP, high accumulated plastic deformation occurs with the formation of a dislocation structure [28]. During deformation, a phase transformation $\alpha'' \rightarrow \beta$ occurs, and a structure with transformed β-zones surrounding α''-regions or vice versa appears. Such microstructural heterogeneity hinders the movement of dislocations—a barrier to slip is created due to the difference in the resistance to deformation of various phases. The transformation is accompanied by the restructuring and reorganization of the dislocation network formed during deformation, some dislocations move or are extinguished, some form dense structures that interfere with the movement of new dislocations [29].

To reduce the hydrogen content to safe concentration, vacuum at a low temperature (e.g., 625 °C [30]) or high-temperature annealing (e.g., at a partial pressure of hydrogen of 100 or 20 mbar and at a temperature of 750 °C [31]) is carried out. In this work, such thermal vacuum treatment to remove hydrogen was carried out after ECAP at a temperature of 550 °C for 1 h [13]. Low-temperature vacuum annealing is used for controlled management of phase composition and structure. Thus, with low-temperature vacuum annealing, the possibility of structure refinement is realized, since in the annealing process, due to the low diffusion mobility of the main alloying elements during the $\beta \rightarrow \alpha$ transformation, the processes of nucleation of new α-phase particles prevail over the pro-

cesses of their growth [32,33]. As a result of annealing, the grain/subgrain size did not change (Figures 8 and 10). At the same time, the material retained high strength with a simultaneous increase in ductility (relative elongation from 2.5 to 5%). A similar effect was observed for the UFG Ti-6Al-4V ELI alloy in the work [34], when annealing at 500 °C for 2 h led to a simultaneous increase in strength and ductility. The authors associated this effect with the restoration of the grain boundary structure to a state closer to equilibrium and the formation of segregations and secondary phases at the grain boundaries, which can additionally contribute to the improvement of the properties of the UFG alloy subjected to annealing. Thus, the preservation of the UFG structure in the alloy after degassing made it possible to obtain a combination of high strength (up to 1500 MPa) and good ductility (relative elongation up to 5%). It should be noted that such a combination of strength and ductility in the Ti-6Al-4V alloy after ECAP treatment was achieved for the first time. A similar level of strength (about 1400 MPa) was achieved after combined deformation treatment, including ECAP and subsequent extrusion, i.e., when achieving a higher degree of deformation [24]. Thus, hydrogen alloying promotes the formation of nanocrystalline and ultrafine-grained structures in titanium alloys obtained as a result of severe plastic deformation at relatively low temperatures and a lower accumulated degree of deformation. In this study, we did not directly compare the mechanical behavior of the samples after ECAP of a hydrogenated and non-hydrogenated alloy, which is the subject of our further research.

5. Conclusions

The results of this study, the purpose of which was to establish the effect of hydrogen as an alloying element on the structural-phase composition, mechanical properties of the TC4 alloy, and the deformability during ECAP to form a UFG structure and increase the strength properties, show the following:

- the use of hydrogen as a temporary alloying element leads to the formation of a thin-plate (from 1 to 4 μm thick) α''-martensitic structure, which does not reduce the deformation capacity of the alloy compared to a hydrogen-free alloy when implementing up to 6 passes ($\varepsilon \sim 4.2$) of ECAP at 600 °C;
- ECAP treatment of the hydrogenated TC4 alloy led to refinement of the grain/subgrain structure to a particle size of 0.15 μm and significant strengthening of the alloy (up to 1550 MPa) with a decrease in relative elongation to 2.5%;
- subsequent vacuum annealing at 550 °C for 1 h after ECAP to remove hydrogen from the solid solution contributed to a reduction in internal elastic stresses due to recovery processes and the preservation of the UFG structure in the alloy.

Thus, the processing of the TC4-0.3H alloy by the ECAP method followed by vacuum annealing made it possible to obtain a tensile strength of 1500 MPa with a relative elongation of 5%, subject to the accumulation of a lower degree of deformation compared with a non-hydrogenated alloy. This combination of strength and ductility was achieved due to the positive effect of reversible hydrogen doping on grain refinement and on phase transformations during the deformation at ECAP.

Author Contributions: Conceptualization, I.P.S. and I.V.A.; methodology, L.R.R. and Z.S.; validation, Y.D., Z.S. and I.V.A.; investigation, L.R.R. and Z.S.; writing—original draft preparation, I.P.S.; writing—review and editing, A.V.P. and Y.D.; visualization, L.R.R. and A.V.P.; supervision, I.V.A.; project administration, I.V.A.; funding acquisition, I.V.A. All authors have read and agreed to the published version of the manuscript.

Funding: This research was funded by the Russian Science Foundation, grant No. 23-43-00041 (https://rscf.ru/project/23-43-00041/ (accessed on 27 Jule 2025)).

Data Availability Statement: The data presented in this study are available on request from the corresponding author.

Conflicts of Interest: The authors declare no conflicts of interest.

References

1. Lütjering, G.; Williams, J.C. *Titanium*; Engineering Materials and Processes; Springer: Berlin, Germany, 2007.
2. Froes, F.H.; Senkov, O.N.; Qazi, J.I. Hydrogen as a temporary alloying element in titanium alloys: Thermohydrogen processing. *Int. Mater. Rev.* **2004**, *29*, 227–245. [CrossRef]
3. Su, Y.; Wang, L.; Luo, L.; Liu, X.; Guo, J.; Fu, H. Investigation of melt hydrogenation on the microstructure and deformation behavior of Ti-6Al-4V alloy. *Int. J. Hydrogen Energy* **2011**, *36*, 1027–1036. [CrossRef]
4. Eliezer, D.; Eliaz, N.; Senkov, O.N.; Froes, F.H. Positive effects of hydrogen in metals. *Mater. Sci. Eng. A* **2000**, *280*, 220–224. [CrossRef]
5. Tal-Gutelmacher, E.; Eliezer, D. High fugacity hydrogen effects at room temperature in titanium based alloys. *J. Alloys Compd.* **2005**, *404–406*, 613–616. [CrossRef]
6. Kim, J.; Plancher, E.; Tasan, C.C. Hydrogenation-induced lattice expansion and its effects on hydrogen diffusion and damage in Ti-6Al-4V. *Acta Mater.* **2020**, *188*, 686–696. [CrossRef]
7. Kudryashova, M.O.; Petrov, S.S.; Yudin, P.E.; Yu, A. Study of the influence of hydrogenation on the destruction and mechanical characteristics of titanium alloy. *Bull. Sib. State Ind. Univ.* **2024**, *4*, 63–71. (In Russian)
8. Senkov, O.N.; Froes, F.H. Thermohydrogen processing of titanium alloys. *Int. J. Hydrogen Energy* **1999**, *24*, 565–576. [CrossRef]
9. Dunstan, M.K.; Vaughn, M.O.; Paramore, J.D.; Butler, B.G.; Kudzal, A.D.; Hemker, K.J. Hemker Optimization of microstructural manipulation and ductility in laser powder bed fusion Ti-6Al-4V through hydrogen heat treatments. *Mater. Sci. Eng. A* **2023**, *873*, 145061. [CrossRef]
10. Li, X.; Jia, G.; Qu, F.; Wu, H.; Chen, J. Ultrafine grain refinement and superplasticity of Ti-55 alloy obtained by hydrogen absorption and desorption. *JMEP* **2018**, *27*, 3472–3477. [CrossRef]
11. Zhao, J.; Ding, H.; Zhao, W.; Jiang, Z. Effects of hydrogen on the hot deformation behaviour of Ti-6Al-4V alloy: Experimental and constitutive model studies. *J. Alloys Compd.* **2013**, *574*, 407–414. [CrossRef]
12. Grabovetskaya, G.P.; Mishin, I.P.; Stepanova, E.N.; Zabudchenko, O.V. Effect of hydrogen on the evolution of the structural-phase state and superplastic properties of an ultrafine-grained alloy of the Ti-Al-V-Mo system. *Phys. Mesomech.* **2022**, *25*, 38–50. (In Russian) [CrossRef]
13. Murzinova, M.A.; Salishchev, G.A.; Afonichev, D.D. Formation of nanocrystalline structure in two-phase titanium alloy by combination of thermohydrogen processing with hot working. *Int. J. Hydrogen Energy* **2002**, *27*, 775–782. [CrossRef]
14. Mulyukov, R.R.; Nazarov, A.A.; Imaev, R.M. Deformational methods of material nanostructuring: Premises, history, state of the art, and prospects. *Russ. Phys. J.* **2008**, *51*, 492–504. [CrossRef]
15. Valiev, R.Z.; Langdon, T.G. The art and science of tailoring materials by nanostructuring for advanced properties using SPD techniques. *Adv. Eng. Mater.* **2010**, *12*, 677–691. [CrossRef]
16. Semenova, I.P.; Saitova, L.R.; Raab, G.I.; Valiev, R.Z. The effect of equal-channel angular pressing on the structure and mechanical behavior of Ti-6Al-4V alloy. *Mater. Sci. Eng. A* **2004**, *387–389*, 805–808. [CrossRef]
17. Agarwal, K.M.; Tyagi, R.K.; Singhal, A.; Bhatia, D. Effect of ECAP on the mechanical properties of titanium and its alloys for biomedical applications. *Mater. Sci. Energy Technol.* **2020**, *3*, 921–927. [CrossRef]
18. Modina, I.M.; Dyakonov, G.S.; Stotskiy, A.G.; Yakovleva, T.V.; Semenova, I. Effect of the Texture of the Ultrafine-Grained Ti-6Al-4V Titanium Alloy on Impact Toughness. *Materials* **2023**, *16*, 1318. [CrossRef]
19. Semenova, I.P.; Modina, Y.M.; Stotskiy, A.G.; Polyakov, A.V.; Pesin, M.V. Fatigue Properties of Ti Alloys with an Ultrafine Grained Structure: Challenges and Achievements. *Metals* **2022**, *12*, 312. [CrossRef]
20. Zhang, J.; Jiang, S.; Jia, Y.; Peng, P.; Li, Y.; Yang, S.; Lu, Z. Microstructure evolution and hydrogen absorption characteristics of gradient-hydrogenated Ti-4.5Al-3V-2Mo-2Fe alloys. *Mater. Design* **2024**, *247*, 113436. [CrossRef]
21. Wu, H.; Dai, T.; Li, T.; Liu, J.; Hu, Q.; Luo, G.; Li, X.; Chen, J. Effect of hydrogenation on fatigue crack growth resistance of diffusion bonded TC4 titanium alloy laminates. *Mater. Charact.* **2024**, *216*, 114311. [CrossRef]
22. Ko, Y.G.; Jung, W.S.; Shin, D.H.; Lee, C.S. Effects of temperature and initial microstructure on the equal channel angular pressing of Ti-6Al-4V alloy. *Scripta Mater.* **2003**, *48*, 197–202. [CrossRef]
23. Rack, H.J.; Qazi, J.; Allard, L.; Valiev, R. Thermal Stability of Severe Plasically Deformed VT-6(Ti-6Al-4V). *Mater. Sci. Forum.* **2008**, *584–586*, 893–898. [CrossRef]
24. Semenova, I.P.; Yakushina, E.B.; Nurgaleeva, V.V.; Valiev, R.Z. Nanostructuring of Ti-alloys by SPD processing to achieve superior fatigue properties. *Int. J. Mater. Res.* **2009**, *100*, 691–1696. [CrossRef]

25. Motyka, M.M.; Sieniawski, J. The influence of initial plastic deformation on microstructure and hot plasticity of α+β titanium alloys. *Mater. Sci. Eng.* **2010**, *41*, 95–103.
26. Zherebtsov, S.; Murzinova, M.; Salishchev, G.; Semiatin, S. Spheroidization of the lamellar microstructure in Ti-6Al-4V alloy during warm deformation and annealing. *Acta Mater.* **2011**, *59*, 4138–4150. [CrossRef]
27. Panin, P.V.; Dzunovich, D.A. Effect of cooling rate on the phase composition and structure of titanium alloy VT6 after hydrogen annealing. *Proc. VIAM* **2017**, *10*, 33–40. (In Russian) [CrossRef]
28. Koujalagi, M.B.; Siddesha, H.S. ECAP of titanium alloy by sever plastic deformation: A review. *Mater. Today Proc.* **2021**, *45*, 71–77. [CrossRef]
29. Sun, J.H. Examination of α″, α′ and ω phases in a β-type titanium–niobium metal. *Mater. Testing* **2022**, *64*, 1720–1732. [CrossRef]
30. Gvozdeva, O.N.; Shalin, A.V.; Stepushin, A.S. Oxide films resistance to hydrogen penetration in VT6 titanium alloy. *IOP Conf. Ser. Mater. Sci. Eng.* **2020**, *889*, 012005. [CrossRef]
31. Schmidt, C.D.; Christ, H.J.; Von Hehl, A. Hydrogen as a Temporary Alloying Element for Establishing Specific Microstructural Gradients in Ti-6Al-4V. *Metals* **2022**, *12*, 1267. [CrossRef]
32. Murzinova, M.A.; Salishchev, G.A.; Afonichev, D.D. Superplasticity of hydrogen-containing VT6 titanium alloy with a submicrocrystalline structure. *Phys. Met. Metallogr.* **2007**, *104*, 195–202. [CrossRef]
33. Motyka, M.M. Martensite Formation and Decomposition during Traditional and AM Processing of Two-Phase Titanium Alloys—An Overview. *Metals* **2021**, *11*, 481. [CrossRef]
34. Valiev, R.Z.; Murashkin, M.Y.; Semenova, I. Grain boundaries and mechanical properties of ultrafine-grained metals. *Metall. Mater. Trans. A* **2010**, *41*, 816. [CrossRef]

Disclaimer/Publisher's Note: The statements, opinions and data contained in all publications are solely those of the individual author(s) and contributor(s) and not of MDPI and/or the editor(s). MDPI and/or the editor(s) disclaim responsibility for any injury to people or property resulting from any ideas, methods, instructions or products referred to in the content.